Geometrical Modeling of Non-Stationary Polarimetric Vehicular Radio Channels

Carlos A. Gutiérrez
Faculty of Science
Universidad Autónoma de San Luis Potosí
San Luis Potosí, Mexico
cagutierrez@ieee.org

Juan C. Ornelas-Lizcano
Faculty of Science
Universidad Autónoma de San Luis Potosí
San Luis Potosí, Mexico
ornelas21@prodigy.net.mx

Matthias Pätzold
Faculty of Engineering and Science
University of Agder
Grimstad, Norway
matthias.paetzold@uia.no

***Abstract*—This paper presents a geometry-based statistical model (GBSM) of polarimetric wideband multipath radio channels for vehicle-to-vehicle (V2V) communications. The proposed model captures the effects of depolarization caused by multipath propagation, and it also accounts for the non-stationary characteristics of wideband V2V channels. This is a novel feature, because the existing polarimetric channel models are built on the assumption that the channel is a wide-sense stationary random process. In the modeling framework described in this paper, the channel depolarization function is given by a linear transformation in the form of a simple rotation matrix. This linear transformation is transparent to the polarization of the transmitting and receiving antennas, and to the geometry of the propagation scenario. Compared to other GBSMs for polarimetric V2V channels, the one proposed here is more flexible, and it simplifies the computation of the channel depolarization function.**

***Index Terms*—Fading channels, mobile communications, non-stationary channels, vehicle-to-vehicle channels, vehicular communications, wave polarization.**

I. Introduction

The growing demand for the services of mobile radio communication systems has fostered a continuous search for novel transmission techniques with high spectral efficiency [1]. In this search, antenna polarization is investigated as an option to double or even triple the channel capacity using compact antenna arrays [2]. However, such an increase in channel capacity can be obtained only when the transmitted signal arrives at the receiver with the same polarization as the receiving antenna. In practice, the polarization matching between the signal and the receiving antenna cannot be guaranteed, due to the depolarization effects caused by multipath propagation [3]. To exploit the full potential of antenna polarization, proper channel models are needed that take into account these depolarization effects. Channel models with such characteristics are known as polarimetric channel models [4].

Initial efforts to characterize the polarimetric multipath radio channel followed an approach in which the channel depolarization function was modeled by a matrix with random coefficients obtained from measured data, or by using ray-tracing simulators, e.g., see [5], [6]. These statistical models provide a closed system (black box) description of the process of channel depolarization. To deepen the understanding of the origin of channel depolarization, Kwon and Stüber proposed a novel geometry-based statistical model (GBSM) of polarimetric channels for single-input single-output (SISO) narrowband vehicle-to-vehicle (V2V) communication systems [7]. This polarimetric channel model was formulated assuming the reflection of waves from interfering objects (IOs) randomly located on the surface of two cylinders. The concept of the conservation-of-polarization (COP) plane was employed as a baseline to determine the rotation of the reflected signal's polarization vector. This modeling approach has been applied to the characterization of other relevant polarimetric channels, e.g., see [8], [9]. However, in the modeling framework of [7]–[9], the rotation of the polarization vector is computed from a pure trigonometrical perspective. Although effective, the methods of [7]–[9] involve lengthy mathematical computations. Moreover, these methods have been applied only to the case of antennas with linear polarization and to the two-cylinders scattering (reflection) propagation model.

In this paper, we revisit the idea of [7] from a vector analysis perspective, which simplifies the calculations considerably. We describe our modeling approach by presenting a new GBSM for polarimetric wideband V2V channels that not only captures the depolarization effects caused by multipath propagation, but also accounts for the non-stationary characteristics of wideband V2V channels. This is an important feature, because measurement data shows that the statistical properties of V2V channels are non-stationary [10]. The existing GBSMs for polarimetric channels do not take into account the channel's non-stationary characteristics (e.g., see [5]–[9]). In the modeling framework of this contribution, the channel depolarization function is given by a linear transformation in the form of a simple rotation matrix. This linear transformation is transparent to the polarization of the transmitting and receiving antennas, and to the geometry of the propagation scenario. Compared to the GBSMs of polarimetric V2V channels presented in [7]–[9], the one proposed here is more flexible and mathematically more tractable.

The remainder of the paper is organized in three sections: The proposed GBSM of non-stationary polarimetric V2V channels is presented in Section II. Our approach for

computing the channel depolarization function is described in Section III. The correlation properties of the proposed polarimetric wideband V2V channel model are analyzed in Section IV to demonstrate that this model is jointly non-wide-sense stationary (non-WSS) in the time and frequency domains. Finally, our conclusions and future research directions are summarized in Section V.

Notation: Throughout the paper, scalar quantities are denoted by variables in plain face, whereas variables in bold face are used for vector quantities. Bold-face variables with a hat (circumflex) are reserved for unit vectors. The operators $(\cdot)^*$, $|\cdot|$, $\|\cdot\|$, $(\cdot)^\dagger$, and $\mathbb{E}\{\cdot\}$ denote the complex conjugate, the absolute value, the Euclidean norm, the transpose, and the statistical expectation, respectively. The scalar product and the vector cross-product between an arbitrary pair of vectors $\mathbf{z}_1$ and $\mathbf{z}_2$ is indicated by $\langle \mathbf{z}_1, \mathbf{z}_2 \rangle$ and $\mathbf{z}_1 \otimes \mathbf{z}_2$, respectively. Vectors are written in spherical coordinates as an ordered triplet (r, θ, ϕ), where r, θ, and ϕ are the vector's magnitude, inclination angle, and azimuth angle, respectively. The inclination and azimuth angles are defined as in [11], [12].

II. The Proposed Geometrical Model of Non-Stationary Polarimetric V2V Channels

A. Geometrical Model of the Propagation Scenario

The polarimetric V2V channel is characterized in this paper considering a SISO communication system, and multipath propagation is supposed to be caused by single interactions of the transmitted signal with $\mathcal{L}$ static (non-moving) interfering objects (IOs). An abstraction of the geometrical configuration of the considered propagation scenario is shown in Fig. 1. In this figure, the initial positions of the moving transmitter (T_X) and receiver (R_X) are indicated by the markers '$\bigtriangledown$', whereas the position of the ℓth IO is indicated by the marker '$\diamondsuit$'. The vectors introduced in Fig. 1 are defined in Table I. The interpretation of the parameters of such vectors is straightforward, but some remarks on the wave vectors $\mathbf{w}_T^\ell$ and $\mathbf{w}_R^\ell$ are worth mentioning. First, $k_0 = 2\pi/\lambda$ is the wavenumber, where λ is the transmitted signal's wavelength. The angles ϑ_T^ℓ and ϑ_R^ℓ characterize the inclination angle-of-departure (IAOD) and the inclination angle-of-arrival (IAOA), respectively, of the signal that travels from the T_X to the R_X via the ℓth IO. Likewise, the angles φ_T^ℓ and φ_R^ℓ characterize the azimuth angle-of-departure (AAOD) and the azimuth angle-of-arrival (AAOA), respectively, of the aforementioned signal. Finally, the wave vector $\widehat{\mathbf{w}}_k^\ell$ and the relative position vector $\mathbf{d}_k^\ell$ are characterized by the same inclination and azimuth angles, because we assume that $\mathbf{w}_k^\ell$ is collinear with $\mathbf{d}_k^\ell$, in such a way that

$$\mathbf{d}_k^\ell = d_k^\ell \widehat{\mathbf{w}}_k^\ell, \quad k \in \{T, R\} \tag{1}$$

where $\widehat{\mathbf{w}}_k^\ell = \widehat{\mathbf{w}}_k / \|\widehat{\mathbf{w}}_k\|$.

The geometrical model of the propagation scenario shown in Fig. 1 has a generic structure that lends itself to the analysis of communication links between vehicles of any type, both terrestrial and airborne. However, in this paper, we focus on terrestrial vehicles. Therefore, we assume that the T_X is initially located at the origin of the coordinate system, whereas the R_X is initially located on the positive x-axis, such that $\mathbf{q}_T^0 = (0,0,0)$ and $\mathbf{q}_R^0 = \mathbf{r}_D = D\widehat{\mathbf{x}}$. We also assume that the IOs are randomly located around the R_X. We model the IAOA ϑ_R^ℓ and the AAOA φ_R^ℓ of $\mathbf{d}_R^\ell$ (and $\mathbf{w}_R^\ell$) by random variables characterized by a joint probability density function (PDF) $p_{\Theta,\Phi}^R(\vartheta, \varphi)$. The magnitude of $\mathbf{d}_R^\ell$ (distance from $\mathbf{q}_R^0$ to $\mathbf{q}_{\text{IO}}^\ell$) is modeled by a function $\mathcal{G}$ of ϑ_R^ℓ and φ_R^ℓ, i.e.,

$$d_R^\ell = \mathcal{G}(\vartheta_R^\ell, \varphi_R^\ell), \quad \mathcal{G} : \mathcal{S} \longmapsto [0, \infty) \tag{2}$$

where $\mathcal{S}$ is the set of points on the sphere of unit radius. The function $\mathcal{G}$ can be specified in different ways. For example, for the cylinder scattering (reflection) propagation model of radius R_c and height h_c [7], $\mathcal{G}$ can be expressed as

$$\mathcal{G}(\vartheta_R^\ell, \varphi_R^\ell) = \begin{cases} \frac{R}{\sin(\vartheta_R^\ell)}, & \forall \varphi_R^\ell, \text{ and } \vartheta_R \in \left[\arctan\left(\frac{h_c}{R_c}\right), 90^\circ\right] \\ 0 & \forall \varphi_R^\ell, \text{ and } \vartheta_R \notin \left[\arctan\left(\frac{h_c}{R_c}\right), 90^\circ\right] \end{cases}. \tag{3}$$

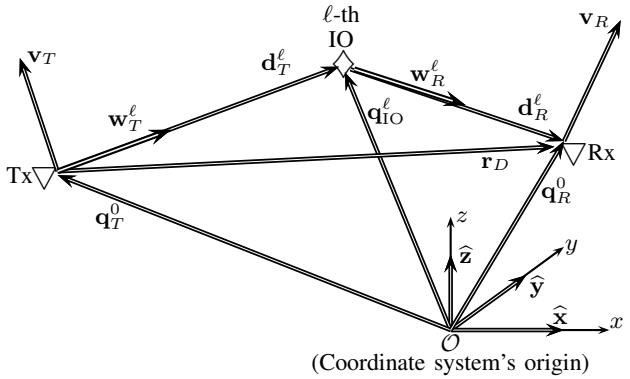

Fig. 1. The reference 2D propagation scenario at time $t_0 = 0$.

TABLE I
Vectors that characterize the geometrical configuration of the propagation scenario.

Description	Form
Initial positions of the moving T_X	$\mathbf{q}_T^0 = (q_T^0, \theta_T^0, \phi_T^0)$
Initial positions of the moving R_X	$\mathbf{q}_R^0 = (q_R^0, \theta_R^0, \phi_R^0)$
Initial position of the R_X as seen from the initial position of the T_X	$\mathbf{r}_D = (D, \theta_D, \phi_D)$
Position of the ℓth IO	$\mathbf{q}_{\text{IO}}^\ell = (q_S^\ell, \theta_S^\ell, \phi_S^\ell)$
Velocity vector of the T_X	$\mathbf{v}_T = (v_T, \gamma_T, \beta_T)$
Velocity vector of the R_X	$\mathbf{v}_R = (v_R, \gamma_R, \beta_R)$
Position of the ℓth IO as seen from the initial position of the moving T_X	$\mathbf{d}_T^\ell = (d_T^\ell, \vartheta_T^\ell, \varphi_T^\ell)$
Initial position of the moving R_X as seen from the ℓth IO	$\mathbf{d}_R^\ell = (d_R^\ell, \pi + \vartheta_R^\ell, \pi + \varphi_R^\ell)$
Wavevector of the signal that travels from the T_X to the ℓth IO	$\mathbf{w}_T^\ell = (k_0, \vartheta_T^\ell, \varphi_T^\ell)$
Wavevector of the signal that travels from the ℓth IO to the R_X	$\mathbf{w}_R^\ell = (k_0, \pi + \vartheta_R^\ell, \pi + \varphi_R^\ell)$

Once the parameters of the vector $\mathbf{d}_R^\ell$ ($\mathbf{w}_R$) are known, those of $\mathbf{d}_T^\ell$ (and $\mathbf{w}_T$) can be determined by noting that $\mathbf{d}_T^\ell = \mathbf{r}_D - \mathbf{d}_R^\ell$ (and taking account of (2)). We model the parameters of the velocity vectors $\mathbf{v}_T$ and $\mathbf{v}_R$ by deterministic quantities.

B. Impulse Response and Transfer Function of the Proposed Polarimetric Wideband Multipath V2V Channel

For the characterization of the impulse response and transfer function of the polarimetric V2V channel, we consider the transmission of an unmodulated carrier having a time-varying electric field intensity equal to

$$\boldsymbol{\mathcal{E}}_T(t) = \exp\{j2\pi f_c t\}\mathbf{E}_T \tag{4}$$

where f_c is the carrier signal's frequency, and $\mathbf{E}_T$ is a complex-valued vector describing the distribution in space of the electric field intensity. This time-invariant vector can be written as

$$\mathbf{E}_T = E_T\widehat{\mathbf{p}}_T. \tag{5}$$

In the previous equation, E_T and $\widehat{\mathbf{p}}_T$ are the transmitting antenna's electric field pattern and the polarization vector, respectively. For an arbitrary elliptical polarization, $\widehat{\mathbf{p}}_T$ can be modeled as a complex-valued unit vector given by

$$\widehat{\mathbf{p}}_T = \widehat{\mathbf{e}}_T^H\cos(\xi_T) + \widehat{\mathbf{e}}_T^V\sin(\xi_T)\exp\{j\eta_T\} \tag{6}$$

where $\widehat{\mathbf{e}}_T^H$ and $\widehat{\mathbf{e}}_T^V$ are real-valued unit vectors, ξ_T is the axial ratio of the transmitting antenna's polarization ellipse, and η_T stands for the phase difference between the scalar components of the real part of $\boldsymbol{\mathcal{E}}_T(t)$ in the directions of $\widehat{\mathbf{e}}_T^H$ and $\widehat{\mathbf{e}}_T^V$ [12]. The unit vectors $\widehat{\mathbf{e}}_T^H$ and $\widehat{\mathbf{e}}_T^V$ are orthogonal to each other, and they are given in such a way that their cross-product $\widehat{\mathbf{e}}_T^H \otimes \widehat{\mathbf{e}}_T^V$ points in the same direction as the transmitted signal's wave vector $\mathbf{w}_T$. To fully specify the orientation of $\widehat{\mathbf{e}}_T^H$ and $\widehat{\mathbf{e}}_T^V$, we assume with reference to Fig. 1 that if the normalized wave vector $\widehat{\mathbf{w}}_T$ is equal to $\widehat{\mathbf{x}}$, then $\widehat{\mathbf{e}}_T^H = \widehat{\mathbf{y}}$ and $\widehat{\mathbf{e}}_T^V = \widehat{\mathbf{z}}$.

The interaction with the ℓth IO produces an attenuation, a phase shift, and a depolarization of the transmitted signal's time-varying electric field intensity $\boldsymbol{\mathcal{E}}_T(t)$. Hence, the time-varying electric field intensity of the signal that arrives at the R_X via the ℓth IO can be expressed as

$$\begin{aligned}\boldsymbol{\mathcal{E}}_R^\ell(t) &= g_\ell E_T\,\mathcal{D}_\ell\{\widehat{\mathbf{p}}_T\} \\ &\quad\times\exp\big\{-j\big(\psi_\ell - 2\pi f_c\big[t-\tau_\ell(t)\big)\big]\big\}.\end{aligned} \tag{7}$$

The scalar variables g_ℓ and ψ_ℓ stand for the attenuation and phase shift produced by the interaction with the IO. We characterize the attenuation factors g_ℓ by positive random variables satisfying the condition $\sum_{\ell=1}^{\mathcal{L}}\mathbb{E}\{|g_\ell|^2\} = 1$. In turn, we model the phase shifts ψ_ℓ by independent and identically distributed (i.i.d.) random variables characterized by a uniform distribution over the interval $[-\pi,\pi)$. The operator $\mathcal{D}_\ell$ designates a linear transformation that rotates the polarization of $\boldsymbol{\mathcal{E}}_T^\ell(t)$. The computation of this linear transformation is the subject of the following section. The time-varying variables $\tau_\ell(t)$ stand for the propagation delay of the ℓth received signal. Assuming the propagation of plane waves and following [13], we model this delay as

$$\tau_\ell(t) = \frac{\langle\mathbf{q}_T^\ell(t),\mathbf{w}_T^\ell\rangle + \langle\mathbf{q}_R^\ell(t),\mathbf{w}_R^\ell\rangle}{k_0\mathcal{C}_0} \tag{8}$$

where $\mathcal{C}_0$ is the speed of light. The time-varying vector $\mathbf{q}_T^\ell(t)$ characterizes the position of the ℓth IO as seen from the instantaneous position of the moving T_X, whereas the time-varying vector $\mathbf{q}_R^\ell(t)$ characterizes the position of the ℓth IO [13] as seen from the instantaneous position of the moving R_X. These two vectors are equal to

$$\mathbf{q}_T^\ell(t) = \mathbf{d}_T^\ell - t\,\mathbf{v}_T \tag{9}$$

$$\mathbf{q}_R^\ell(t) = \mathbf{d}_R^\ell + t\,\mathbf{v}_R. \tag{10}$$

The total received signal detected by the receiving antenna can be expressed as

$$\mathcal{Y}(t) = \sum_{\ell=1}^{\mathcal{L}}\Big\langle\boldsymbol{\mathcal{E}}_R^\ell(t),\mathbf{A}_R^*\Big\rangle \tag{11}$$

where $\mathbf{A}_R = A_R\widehat{\mathbf{a}}_R$ is known as the vector effective length of the receiving antenna [12]. The scalar component of $\mathbf{A}_R$, which is denoted by A_R, has units of distance, and therefore differs from the electric field pattern of the receiving antenna. However, the vector component of $\mathbf{A}_R$, denoted by $\widehat{\mathbf{a}}_R$, is equal to the receiving antenna's polarization vector. Thus, for an arbitrary elliptical polarization, we can characterize $\widehat{\mathbf{a}}_R$ as a complex-valued unit vector given by

$$\widehat{\mathbf{a}}_R = \widehat{\mathbf{e}}_R^H\cos(\xi_R) + \widehat{\mathbf{e}}_R^V\sin(\xi_R)\exp\{j\eta_R\}. \tag{12}$$

The real-valued vectors $\widehat{\mathbf{e}}_R^H$ and $\widehat{\mathbf{e}}_R^V$ are chosen in a similar way as $\widehat{\mathbf{e}}_T^H$ and $\widehat{\mathbf{e}}_T^V$. The sole difference is that $\widehat{\mathbf{e}}_R^H$ and $\widehat{\mathbf{e}}_R^V$ are given such that their cross-product, $\widehat{\mathbf{e}}_R^H \otimes \widehat{\mathbf{e}}_R^V$, and the wave vector $\widehat{\mathbf{w}}_R^\ell$ point in opposite directions. We assume that if the normalized wave vector $\widehat{\mathbf{w}}_R$ is equal to $\widehat{\mathbf{x}}$, then $\widehat{\mathbf{e}}_R^H = -\widehat{\mathbf{y}}$ and $\widehat{\mathbf{e}}_R^V = \widehat{\mathbf{z}}$. The variables ξ_R and η_R introduced in (12) have a similar meaning as their transmitting antenna's counterparts introduced in (6). By substituting (7) into (11), we find

$$\begin{aligned}\mathcal{Y}(t) &= \sum_{\ell=1}^{\mathcal{L}}\langle\mathcal{D}_\ell\{\widehat{\mathbf{p}}_T\},\widehat{\mathbf{a}}_R^*\rangle\,g_\ell A_R E_T \\ &\quad\times\exp\big\{-j\big(\psi_\ell - 2\pi f_c\big[t-\tau_\ell(t)\big]\big\}.\end{aligned} \tag{13}$$

From the previous result, it follows that the polarimetric channel impulse response (CIR) can be expressed in the complex baseband equivalent as

$$\begin{aligned}u(t;\tau) &= \sum_{\ell=1}^{\mathcal{L}}\langle\mathcal{D}_\ell\{\widehat{\mathbf{p}}_T\},\widehat{\mathbf{a}}_R^*\rangle\,g_\ell A_R E_T \\ &\quad\times\exp\big\{-j\big[\psi_\ell + 2\pi f_c\tau_\ell(t)\big]\big\}\delta(\tau-\tau_\ell(t)).\end{aligned} \tag{14}$$

Hence, the polarimetric channel transfer function (CTF) $U(t;f) \triangleq \int_{-\infty}^{\infty}u(t;\tau)\exp\{-j2\pi f\tau\}\,\mathrm{d}\tau$ is equal to

$$\begin{aligned}U(t;f) &= \sum_{\ell=1}^{\mathcal{L}}\langle\mathcal{D}_\ell\{\widehat{\mathbf{p}}_T\},\widehat{\mathbf{a}}_R^*\rangle\,g_\ell A_R E_T \\ &\quad\times\exp\big\{-j\big[\psi_\ell + 2\pi(f_c+f)\tau_\ell(t)\big]\big\}.\end{aligned} \tag{15}$$

III. Characterization of the Channel Depolarization Functions

The problem to be solved is to find the linear transformation $\mathcal{D}_\ell$ that characterizes the rotation of $\widehat{\mathbf{p}}_T$ due to the interaction with the ℓth IO. Such a linear transformation should be computed following the fundamental principles of electromagnetic (EM) wave propagation and taking into account the geometrical configuration of the propagation scenario. To solve this problem, we assume that the transmitted signal interacts with the IOs by the mechanism of reflection. We can therefore apply the concept of the COP plane [7], [8] (a.k.a. the incident plane [11]) to determine the orientation of $\widehat{\mathbf{p}}_T$ after the reflection by the ℓth IO.

The COP plane can be defined as the plane spanned by the wave vectors of the transmitted (incident) and received (reflected) signals [11]. The reflection of the transmitted signal by the ℓth IO is illustrated in Fig. 2 from the perspective of the COP plane. In this figure, the signal's angle of incidence and angle of reflection are denoted by Θ_i and Θ_r, respectively, whereas

$$\Phi_\ell = \cos^{-1}\left(\langle \widehat{\mathbf{w}}_T^\ell, \widehat{\mathbf{w}}_R^\ell \rangle\right) \tag{16}$$

stands for the shortest angle between $\widehat{\mathbf{w}}_T^\ell$ and $\widehat{\mathbf{w}}_R^\ell$. In the COP plane, signals reflected by perfect conductors and lossless dielectrics maintain the polarization of the incident wave. However, the polarization vector of the reflected signal, $\widehat{\mathbf{p}}_R^\ell$, has a different orientation in space than the polarization vector of the incident signal, $\widehat{\mathbf{p}}_T^\ell$, because the direction of propagation of these signals is different [11]. This is illustrated in Fig. 2, where both $\widehat{\mathbf{p}}_T^\ell$ and $\widehat{\mathbf{p}}_R^\ell$ are parallel to the COP plane, but point in different directions to fulfill the condition of perpendicularity with the corresponding wave vector, and to satisfy the right-hand rule (this latter requirement was neglected in the diagram of the COP plane shown in [7]).

Based on the propagation mechanism described above, the orientation of the received signal's polarization vector is computed in [7]–[9] by applying tools of pure trigonometry. Although effective, the trigonometrical approach of [7]–[9] complicates the computation of the rotated polarization vectors. Another limitation of [7]–[9] is that the obtained results are valid only for a particular geometrical configuration of the propagation scenario. We bypass such limitations by approaching the problem from a vector analysis perspective. To that end, we note from Fig. 2 that the polarization vector $\widehat{\mathbf{p}}_R^\ell$ can be obtained from $\widehat{\mathbf{p}}_T^\ell$ by a simple rotation about the normal to the COP plane. Specifically, to obtain $\widehat{\mathbf{p}}_R^\ell$, we only need to conduct a counter-clockwise rotation of $\widehat{\mathbf{p}}_T^\ell$ by an angle Φ_ℓ about the unit vector

$$\widehat{\mathbf{n}}_\ell = \frac{\widehat{\mathbf{w}}_T^\ell \otimes \widehat{\mathbf{w}}_R^\ell}{\|\sin(\Phi_\ell)\|} = \widehat{\mathbf{x}} N_\ell^x + \widehat{\mathbf{y}} N_\ell^y + \widehat{\mathbf{z}} N_\ell^z \tag{17}$$

(cf. Fig. 2). Hence, for the case of non-collinear wave vectors, the linear transformation $\mathcal{D}_\ell$, which accounts for the effects of channel depolarization caused by wave reflection, can be modeled in a compact and simple form as

$$\mathcal{D}_\ell\{\widehat{\mathbf{p}}_T^\ell\} \;=\; \mathbf{M}_\ell \widehat{\mathbf{p}}_T^\ell \tag{18}$$

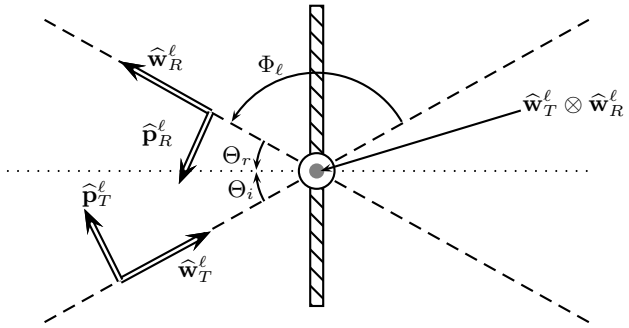

Fig. 2. Geometry of the reflection of an EM wave in the COP plane.

where $\mathbf{M}_\ell$ is a rotation matrix defined for a counter-clockwise rotation by an angle Ψ_ℓ about an axis in the direction of $\widehat{\mathbf{n}}_\ell$.[1] A rotation matrix with these characteristics already exists [14], which is given by (20) at the top of the next page. It is worth noting that the evaluation of (17) produces a singularity for collinear wave vectors. However, if $\widehat{\mathbf{w}}_T^\ell$ is collinear to $\widehat{\mathbf{w}}_R^\ell$, then it means that the transmitted signal is blocked by the IO ($\Phi_\ell = \pi$), or that the signal reaches the R_X before the IO ($\Phi_\ell = 0$). Taking account of (18), we can rewrite (15) as

$$\begin{aligned} U(t;f) \;&=\; \sum_{\ell=1}^{\mathcal{L}} (\widehat{\mathbf{p}}_T^\ell)^\dagger \, \mathbf{M}_\ell^\dagger \, \widehat{\mathbf{a}}_R^* \, g_\ell A_R E_T \\ &\quad \times \exp\left\{-j\left[\psi_\ell + 2\pi(f_c + f)\tau_\ell(t)\right]\right\}. \end{aligned} \tag{19}$$

The mathematical model of the polarimetric CTF given by (19) is similar to the one proposed in [6]. However, the elements of the depolarization matrix $\mathbf{M}_\ell$ are modeled in [6] by i.i.d. random variables whose statistical distribution does not take into account the geometry of the propagation scenario. This contrasts with (20), where the geometry of the propagation scenario is embedded by means of Φ_ℓ and $\widehat{\mathbf{n}}_\ell$.

IV. Correlation Properties of the Proposed Geometrical Polarimetric V2V Channel Model

For the analysis of the correlation properties of the proposed geometrical polarimetric V2V channnel model, we consider the definition of the four-dimensional time-frequency correlation function (4D-TFCF) given in [15] as follows

$$\mathcal{R}(t, f; \Delta t, \Delta f) = \mathbb{E}\{U^*(t - \Delta t; f) U(t; f + \Delta f)\}. \tag{22}$$

Under the assumptions discussed in Section II, we obtain by a direct evaluation of (22) the result presented in (21) at the top of the next page, where

$$f_D^0 \;=\; \frac{\langle \mathbf{v}_T, \widehat{\mathbf{w}}_T \rangle - \langle \mathbf{v}_R, \widehat{\mathbf{w}}_R \rangle}{\lambda} \tag{23}$$

$$G_D \;=\; \frac{\langle \mathbf{d}_T, \widehat{\mathbf{w}}_T \rangle + \langle \mathbf{d}_R, \widehat{\mathbf{w}}_R \rangle}{\mathcal{C}_0}. \tag{24}$$

[1] Equation (18) is given under the assumption that the polarization vector $\widehat{\mathbf{p}}_T^\ell$ is arranged in the form of a column vector. The same consideration will be made for $\widehat{\mathbf{a}}_R^\ell$.

$$\mathbf{M}_\ell = \begin{bmatrix} \cos\Phi_\ell + (N_\ell^x)^2(1-\cos\Phi_\ell) & N_\ell^x N_\ell^y(1-\cos\Phi_\ell) - N_z\sin\Phi_\ell & N_\ell^x N_\ell^z(1-\cos\Phi_\ell) + N_y\sin\Phi_\ell \\ N_\ell^x N_\ell^y(1-\cos\Phi_\ell) + N_z\sin\Phi_\ell & \cos\Phi_\ell + (N_\ell^y)^2(1-\cos\Phi_\ell) & N_\ell^y N_\ell^z(1-\cos\Phi_\ell) - N_x\sin\Phi_\ell \\ N_\ell^x N_\ell^z(1-\cos\Phi_\ell) - N_y\sin\Phi_\ell & N_\ell^y N_\ell^z(1-\cos\Phi_\ell) + N_x\sin\Phi_\ell & \cos\Phi_\ell + (N_\ell^z)^2(1-\cos\Phi_\ell) \end{bmatrix} \tag{20}$$

$$\mathcal{R}(t,f;\Delta t,\Delta f) = \int_0^{2\pi}\int_0^{\pi} \left|(\widehat{\mathbf{p}}_T)^\dagger\,\mathbf{M}^\dagger\,\widehat{\mathbf{a}}_R^*\right|^2 (A_R E_T)^2 \exp\left\{j2\pi\left[\Delta t f_D^0 \frac{f_c+f}{f_c} - \Delta f\left(G_D - t\frac{f_D^0}{f_c}\right)\right]\right\} p_{\Theta,\Phi}^R(\vartheta,\varphi)\,\mathrm{d}\vartheta\,\mathrm{d}\varphi \tag{21}$$

The scalar variable f_D^0 can be identified as the Doppler shift of the carrier signal, whereas G_D is a function that characterizes the propagation delay of signals transmitted in all directions at the time instant $t = 0$. In turn, the vector variables $\mathbf{d}_k$ and $\widehat{\mathbf{w}}_k$ are given as $\mathbf{d}_k = \left(d_k, \vartheta_k, \varphi_k\right)$ and

$$\widehat{\mathbf{w}}_k^\ell = \widehat{\mathbf{x}}\sin\vartheta_k\cos\varphi_k + \widehat{\mathbf{y}}\sin\vartheta_k\sin\varphi_k + \widehat{\mathbf{z}}\cos\vartheta_k \tag{25}$$

for $k \in \{T, R\}$. We note that the 4D-TFCF is evaluated in (21) only with respect to the joint PDF of the IAOA ϑ_R and the AAOA φ_R, because the IAOA ϑ_T and the AAOA φ_T can be modeled as functions of the former pair of angles, as explained in [13] for the case of a two-dimensional propagation scenario.

Three remarks about the results presented in (21) are as follows: First, we can conclude that the proposed geometrical polarimetric V2V channel model is non-stationary in both the time and frequency domain, because its 4D-TFCF depends on the time variable t and the frequency variable f. Second, we note that the 4D-TFCF in (21) is a generalization with respect to polarimetric channels of the result obtained in [13] for the correlation function of co-polarized wideband V2V channels. Third, while not shown in this paper, the depolarization function has an indirect influence on the non-stationary characteristics of the proposed polarimetric channel model. The depolarization function has an impact on the shape of the 4D-TFCF, and therefore on the decorrelation properties, coherence intervals, and stationary intervals of the channel.

V. Conclusions and Future Work

In this paper, we have shown that the effects of channel depolarization produced by the reflection of waves from IOs can be modeled by a linear transformation in the form of a simple rotation matrix. The elements of such a rotation matrix are defined considering the geometrical configuration of the propagation environment, and conducting simple vector algebra operations between the wave vectors of the transmitted and received signals. We presented a new GBSM for polarimetric wideband V2V channels that is transparent to the polarization of the transmitting and receiving antennas, and we derived an expression for the 4D-TFCF of this new model. The obtained results show that its second-order statistics are non-WSS in both time and frequency. This is a desirable feature, as empirical investigations have shown that the V2V channel do not fulfill the WSS condition. Our approach to the geometrical modeling of polarimetric channels has been described in detail in this paper. However, further work is needed to validate the geometrical non-stationary polarimetric V2V channel model presented here. For a future paper, we leave the analysis of the cross-polarization discrimination, the derivation of compact closed-form expressions for the 4D-TFCF, and the comparison with other polarimetric V2V channel models, e.g., that of Kwon and Stüber. In addition, we leave for future work the extension of our modeling approach with respect to the mechanisms of wave propagation by scattering and diffraction.

Acknowledgment

This work was financed in part by COPOCYT (Consejo Potosino de Ciencia y Tecnología).

References

[1] A. Gupta and R. K. Jha, "A survey of 5G network: Architecture and emerging technologies," *IEEE Access*, vol. 3, pp. 1206–1232, 2015.

[2] A. Molisch, *Wireless Communications*. Chichester, UK: John Wiley and Sons, 2005.

[3] T. Brown, E. D. Carvalho, and P. Kyritsi, *Practical Guide to the MIMO Mobile Radio Channel*. New York: John Wiley and Sons, 2012.

[4] C. Gustafson, D. Bolin, and F. Tufvesson, "Modeling the polarimetric mm-wave propagation channel using censored measurements," in *Proc. 2016 IEEE Global Communications Conference (GLOBECOM)*, Washington, DC, USA, Dec. 2016, pp. 1–6.

[5] C. Oestges, V. Erceg, and A. Paulraj, "Propagation modeling of MIMO multipolarized fixed wireless channels," *IEEE Trans. Veh. Technol.*, vol. 53, no. 3, pp. 644–654, May 2004.

[6] M. Shafi *et al.*, "Polarized MIMO channels in 3-D: Models, measurements and mutual information," vol. 24, no. 3, pp. 514–527, Mar. 2006.

[7] S.-C. Kwon and G. L. Stüber, "Geometrical theory of channel depolarization," *IEEE Trans. Veh. Technol.*, vol. 60, no. 8, pp. 3542–3556, 2011.

[8] S.-C. Kwon, G. L. Stüber, A. V. López, and J. Papapolymerou, "Geometrically based statistical model for polarized body-area-network channels," *IEEE Trans. Veh. Technol.*, vol. 62, no. 8, pp. 3518–3530, 2013.

[9] R. He, B. Ai, G. L. Stüber, and Z. Zhong, "Geometrical-based statistical modeling for polarized MIMO mobile-to-mobile channels," *IEEE Trans. Antennas Propag.*, vol. 66, no. 8, pp. 4213–4227, Aug. 2018.

[10] C. Mecklenbrauker *et al.*, "Vehicular channel characterization and its implications for wireless system design and performance," *Proc. IEEE*, vol. 99, no. 7, pp. 1189–1212, Jul. 2011.

[11] N. Ida, *Engineering Electromagnetics*, 2nd ed. New York: Springer-Verlag, 2004.

[12] W. L. Stutzman and G. A. Thiele, *Antenna Theory and Design*, 2nd ed. New Jersey: John Wiley and Sons, 1998.

[13] C. A. Gutiérrez *et al.*, "Geometry-based statistical modeling of non-WSSUS mobile-to-mobile Rayleigh fading channels," *IEEE Trans. Veh. Technol.*, vol. 67, no. 1, pp. 362–377, Jan. 2018.

[14] S. L. Altmann, *Rotations, Quaternions, and Double Groups*. New York: Dover Publications, 2005.

[15] G. Matz, "On non-WSSUS wireless fading channels," *IEEE Trans. Wireless Commun.*, vol. 4, no. 5, pp. 2465–2478, Sep. 2005.